

## Kinetic Evidence for Duplicity in Ion Transport

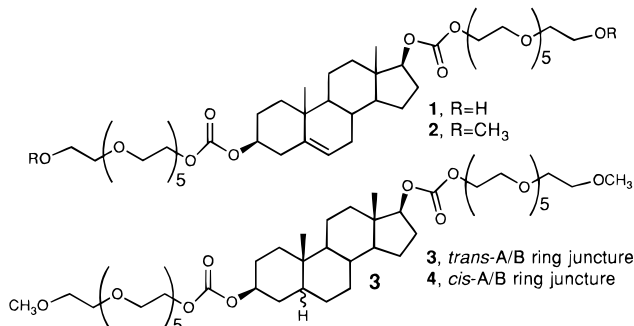
Gang Deng, Manette Merritt, Keiji Yamashita, Vaclav Janout, Andrzej Sadownik, and Steven L. Regen\*

Department of Chemistry and Zettlemoyer Center for Surface Studies, Lehigh University  
Bethlehem, Pennsylvania 18015

Received August 8, 1995

Revised Manuscript Received February 20, 1996

In recent years, there has been growing interest in the design and synthesis of molecules that mimic the structure and function of naturally-occurring ionophores.<sup>1</sup> While considerable attention has focused on structure/activity relationships, the possibility that such compounds may operate through multiple mechanisms has not, to the best of our knowledge, previously been considered. In this paper, we report the results of a kinetic investigation of the ion transport properties of four sterol-oligo-(ethylene glycol) conjugates that have been modeled after the heptaene macrolide antibiotic, Amphotericin B.<sup>2</sup> Specifically, we report the activity of **1**, **2**, **3**, and **4** in promoting the transport of Na<sup>+</sup> across egg phosphatidylcholine bilayers as a function of their membrane concentration.<sup>3</sup> Our kinetic results not only provide compelling evidence for the existence of *two discrete forms of an active ionophore in each case* but also serve as a cautionary note for interpreting ionophoric activity based on single-concentration experiments.



In this work, we have used <sup>23</sup>Na NMR spectroscopy as a means of monitoring Na<sup>+</sup> transport.<sup>1a</sup> In brief, a solution of NaCl plus a paramagnetic shift reagent is added to an egg PC dispersion (1000 Å diameter, large unilamellar vesicles) that has been prepared in aqueous LiCl. If the shift reagent is confined to the external aqueous phase, then the Na<sup>+</sup> that enters the vesicular compartments will appear as a separate (unshifted) resonance. An obligatory Li<sup>+</sup> exit (antiport) and/or Cl<sup>-</sup> entry (symport), which is necessary in order to maintain electroneutrality on both sides of the membrane, permits the complete discharge of the concentration gradient and the transmembrane

(1) (a) Pregel, M. J.; Jullien, L.; Canceill, J.; Lacombe, L.; Lehn, J. M. *J. Chem. Soc., Perkin Trans. 2*, **1995**, 417. (b) Kragten, U. F.; Roks, F. M.; Nolte, R. J. M. *J. Chem. Soc., Chem. Commun.* **1985**, 1275. (c) Nakano, A.; Xie, Q.; Mallen, J. V.; Echeegoyen L.; Gokel, G. W. *Ibid.* **1990**, 112, 1287. (d) Tabushi, I.; Kuroda, Y.; Yokota *Tetrahedron Lett.* **1982**, 23, 4601. (e) Lear, J. D.; Wassermann, Z. R.; DeGrado, W. F. *Science* **1988**, 1177. (f) Fyles, T. M.; James, T. D.; Kaye, K. C. *J. Am. Chem. Soc.* **1993**, 115, 12315. (g) Stankovic, C. J.; Heinemann, S. H.; Schreiber, S. L. *J. Am. Chem. Soc.* **1990**, 112, 3702. (h) Kobuke, Y.; Ueda, K.; Sokabe, M. *J. Am. Chem. Soc.* **1992**, 114, 7618. (i) Menger, F. M.; Davis, D. S.; Persichetti, R. A.; Lee, J. J. *J. Am. Chem. Soc.* **1990**, 112, 2451. (j) Ghadiri, M. R.; Granja, J. R.; Buehler, L. K. *Nature* **1994**, 369, 301. (k) Voyer, N.; Robitaille, M. *J. Am. Chem. Soc.* **1995**, 117, 6599. (l) Murillo, O.; Watanabe, S.; Nakano, A.; Gokel, G. W. *J. Am. Chem. Soc.* **1995**, 117, 7665.

(2) Stadler, E.; Dedek, P.; Yamashita, K.; Regen, S. L. *J. Am. Chem. Soc.* **1994**, 116, 6677.

(3) Compounds **2**, **3**, and **4** were synthesized using procedures that were very similar to those previously described for **1**.<sup>2</sup>

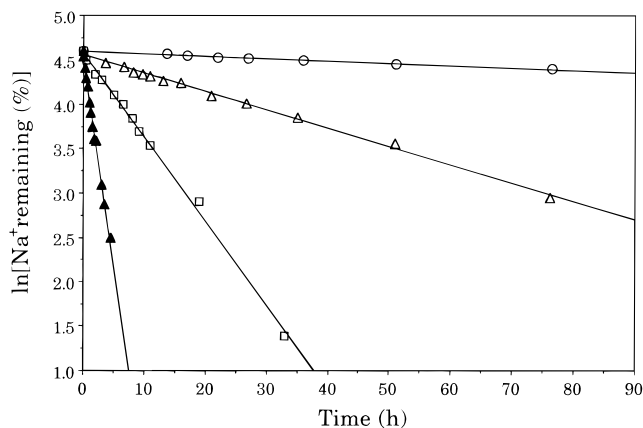


**Figure 1.** Typical first-order plots of percentage of Na<sup>+</sup> that remains to enter egg phosphatidylcholine vesicles containing (O) **1**, (Δ) **2**, (□) **3**, and (▲) **4** mol % of **1** at 25 °C.

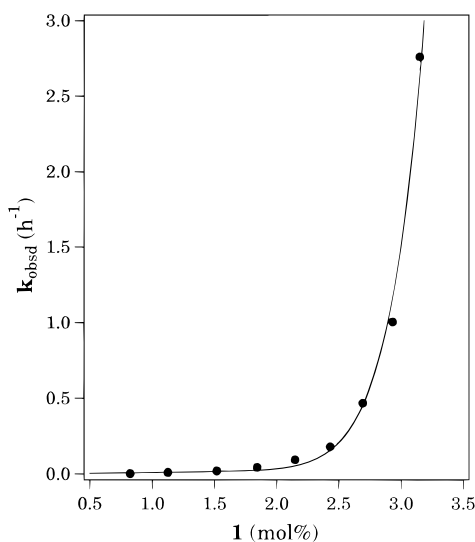


**Figure 2.** Plot of  $k_{\text{obsd}}$  as a function of mol % of **1**. The smooth curve represents a nonlinear least squares fit of the data based on eq 2.

potential that drives the ion transport.<sup>4</sup> Specific protocols that were used in this work were similar to those previously described.<sup>2</sup> Under our experimental conditions, the rate of Na<sup>+</sup> entry was found to obey pseudo first-order kinetics where  $d[\text{Na}^+]/dt = k_{\text{obsd}}[\text{Na}^+]$ ; typical plots that were obtained are shown in Figure 1. A plot of the  $k_{\text{obsd}}$  versus the mol % of **1** is presented in Figure 2.<sup>5</sup>

The strong dependency of  $k_{\text{obsd}}$  on the concentration of **1** indicates the involvement of sterol aggregates in the transport process.<sup>2</sup> If each of these aggregates is composed of  $n$  ionophore molecules, and if the dissociation constant that defines the aggregate–monomer equilibrium within the membrane is represented by  $K$ , then it can be readily shown that  $k_{\text{obsd}}$  will depend upon  $K$ , the concentration of membrane-bound ionophore  $[\text{Ionophore}]$ , and an intrinsic rate constant ( $k$ ) that characterizes the aggregate-mediated transport according to eq 1.<sup>2</sup> When the majority of ionophores exists as membrane-bound

$$k_{\text{obsd}} = \frac{k[\text{Ionophore}]^n}{K} \quad (1)$$

(4) Preliminary <sup>7</sup>Li<sup>+</sup> NMR studies carried out with **1** indicate that the rate of Li<sup>+</sup> exit is very similar to the rate of Na<sup>+</sup> entry. Vesicle dispersions were used directly after extrusion; all NMR measurements were made at 25 °C.

(5) Reproducibility of rate constants ( $k_{\text{obsd}}$ ) was ±8%.

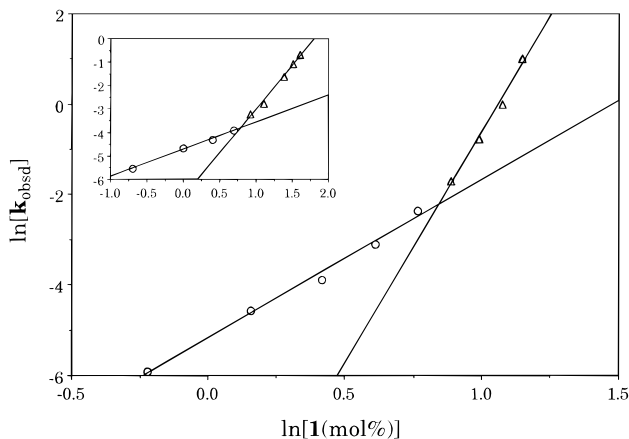


**Figure 3.** Plot of  $\ln(k_{\text{obsd}})$  versus  $\ln[I \text{ (mol \%)}]$ . Two different symbols have been used to designate two linear regions that are apparent. The inset shows similar data for **2**. Very similar data has been obtained for **3** and **4** (not shown).

**Table 1.** Values of  $k_1$ ,  $k_n$ , and  $n$  Obtained from Curve Fitting of Equation 2

ionophore	$10^2 k_1$ ( $\text{h}^{-1} \text{mol \%}^{-1}$ )	$10^6 k_n$ ( $\text{h}^{-1} \text{mol \%}^{-n}$ )	$n$
<b>1</b>	$1.15 \pm 0.42$	$2.8 \pm 0.15$	12
<b>2</b>	$0.50 \pm 0.27$	$738 \pm 67$	4
<b>3</b>	$1.24 \pm 0.33$	$109 \pm 5.7$	6
<b>4</b>	$1.62 \pm 0.31$	$7.8 \pm 0.26$	8

monomer, its “analytical” concentration (i.e., the total concentration that is present in the dispersion) can be used to approximate  $[Ionophore]$ . Under such conditions, a plot of  $\ln(k_{\text{obsd}})$  versus  $\ln[ionophore]$  is expected to yield a straight line with a slope that corresponds to the aggregation number,  $n$ . Figure 3 shows such a plot for **1**. What is readily apparent from this figure is the presence of *two distinct linear regions*. Exactly analogous results were obtained for **2**, **3**, and **4**.

If ion transport is governed by two distinct processes, one that is first-order with respect to the ionophore concentration (monomer-active) and one that has an  $n$ -th order dependency on the ionophore concentration (aggregate-active), then the observed rate would be expected to obey eq 2, where  $k_n = k/K$

$$d[\text{Na}^+]/dt = (k_1[ionophore] + k_n[ionophore]^n)[\text{Na}^+] = k_{\text{obsd}}[\text{Na}^+] \quad (2)$$

and  $k_1$  is the first-order rate constant for the monomer-active form. By use of eq 2, a nonlinear least squares fit of  $k_{\text{obsd}}$  as a function of ionophore concentration yields values of  $k_1$ ,  $k_n$ , and  $n$  for **1**, **2**, **3**, and **4** which are shown in Table 1. The similarity of  $k_1$  within this series of sterol conjugates implies that the presence of terminal hydroxyls groups, the presence of a double bond within the B-ring of the sterol, and the stereochemistry of the A/B ring juncture have little influence on monomer activity. Although it would be of interest to compare the intrinsic activities ( $k$ ) of **1–4** in their aggregated state, our kinetic analysis does not permit such a comparison to be made since the kinetic and thermodynamic components of  $k_n$  (i.e.,  $k$  and  $K$ ) cannot be separated.

What are the two pathways for ion transport that are associated with these synthetic ionophores? A likely possibility for a monomer-active species is that it functions as a carrier, i.e., it shuttles ions from one side of the bilayer to the other. On the basis of analogy to Amphotericin B, an aggregate-active form is more likely to involve a channel (or pore) mechanism.<sup>6</sup> Although conductance experiments can distinguish between carriers and channels, such measurements do not have sufficient sensitivity for determining the ion flux associated with **1–4**.<sup>7</sup> For this reason, we have chosen what is considered by most researchers to be “the next best experiment”, i.e., to measure ionophoric activity in fluid- versus gel-phase vesicles.<sup>6</sup> In brief, a carrier is expected to show greatly diminished activity in gel-phase membranes since the rate of diffusion across the bilayer is significantly reduced. In contrast, the activity of a membrane-spanning ion channel is expected to be almost independent of membrane viscosity since transbilayer movement of the ionophore is not required. A recent study lends strong support for this hypothesis.<sup>1a</sup> In particular, comparison of the rates of  $\text{Na}^+$  transport across egg PC (fluid phase, 25 °C) and 1,2-dipalmitoyl-*sn*-glycero-3-phosphocholine (DPPC) membranes (gel phase, 25 °C) has confirmed the carrier mechanism for the natural ionophore monensin and a channel mechanism for gramicidin.<sup>1a</sup>

In preliminary studies, we have found that the use of a “low” concentration (1 mol %) of **4** within gel-phase vesicles (DPPC, 25 °C) did not result in detectable  $\text{Na}^+$  transport after 168 h, i.e.,  $k_{\text{obsd}} \ll 1 \times 10^{-3} \text{ h}^{-1}$ . In contrast, analogous fluid-phase egg PC (25 °C) vesicles gave a value of  $k_{\text{obsd}} = 11.2 \times 10^{-3} \text{ h}^{-1}$ . Similar experiments that were carried out using a relatively “high” concentration of **4** (2.5 mol %) in gel-phase DPPC vesicles (25 °C) gave  $k_{\text{obsd}} = 35 \times 10^{-3} \text{ h}^{-1}$ ; in fluid-phase egg PC (25 °C) a value of  $k_{\text{obsd}} = 62 \times 10^{-3} \text{ h}^{-1}$  was obtained. These results are fully consistent with a dominant carrier mechanism at low ionophore concentrations and a channel mechanism at high concentrations. The fact that both active forms can discriminate between  $\text{Na}^+$  and shift reagent  $[\text{Dy}(\text{P}_3\text{O}_{10})_2]^{7-}$  (i.e., only  $\text{Na}^+$  crosses the bilayer) further indicates that neither form induces major defects within the membrane.

The existence of two active forms of **1–4** clearly demonstrates that transport behavior of relatively simple ionophores can be much richer in complexity than previously realized. It also shows that mechanistic interpretations based on single-concentration experiments should be viewed with extreme caution.

**Acknowledgment.** We are grateful to Dr. Francois Kezdy (The Upjohn Company) for valuable discussions and to the National Institutes of Health (PHS Grant AI28220) for support of this research.

**Supporting Information Available:** One table containing the complete set of kinetic data for **1**, **2**, **3**, and **4**, analytical data for **2**, **3**, and **4**, and experimental procedures for performing the  $^{23}\text{Na}^+$  measurements (4 pages). This material is contained in libraries on microfiche, immediately follows this article in the microfilm version of the journal, can be ordered from the ACS, and can be downloaded from the Internet; see any current masthead page for ordering information and Internet access instructions.

JA9526877

(6) Stein, W. D. *Channels, Carriers, and Pumps: An Introduction to Membrane Transport*; Academic Press: New York, 1990.

(7) Lear, J. D.; Wasserman, Z. R.; DeGrado, W. F. *Science* **1988**, 1177.